

## TRITON/NEWT CALCULATION OF THE CORAIL ASSEMBLY FOR PLUTONIUM RECYCLING IN PWR

**Francesco Ganda, Miodrag Milosevic and Ehud Greenspan**  
University of California at Berkeley, Berkeley CA 94720-1730 USA  
gandaf@nuc.berkeley.edu

**Temitope Taiwo**  
Argonne National Laboratory,  
9700 South Cass Avenue Argonne,  
IL 60439, USA

### ABSTRACT

The TRITON/NEWT code sequence of SCALE 5.1 and associated cross section libraries are benchmarked in this work against WIMS8 and APOLLO2 for the plutonium-bearing CORAIL assembly. The CORAIL assembly is designed for the multi-recycling of plutonium in PWR, using an heterogeneous configuration of UO<sub>2</sub> and MOX fuel pins. The heterogeneity makes the modeling of this assembly type particularly challenging. TRITON/NEWT shows a satisfactory agreement on the evolution of  $k_{\infty}$  with burnup, on the assembly pin-wise power peaking and on the burnup dependent concentration of most of the minor actinides. An exception is found to be the burnup-dependent evolution of <sup>242m</sup>Am, which shows discrepancies of up to 60%. The reason was traced to the branching ratio of the (n,γ) reaction of <sup>241</sup>Am. Upon modification of the probability of formation of <sup>242m</sup>Am from the default 16.2% to 10% (used by WIMS8) in the ORIGEN-S binary libraries, the large discrepancy in the concentration of <sup>242m</sup>Am disappeared. It is also found that by slightly varying the group structure of the standard 44-UOX library of SCALE 5.1 it is possible to get closer agreement with the results obtained using the standard 238-group library.

*Key Words:* TRITON, NEWT, NITAWL, CENTRM, MOX, CORAIL, <sup>241</sup>Am BRANCHING RATIO

### 1. INTRODUCTION

The CORAIL is a 17x17 PWR fuel assembly design having 264 fuel rods of which 84 are MOX pins and the remaining 180 are UO<sub>2</sub> pins using enriched uranium. The main aim of the CORAIL assembly is to allow for multi-recycling of plutonium in PWR [1]. It has been shown capable of stabilizing the plutonium inventory without requiring any modification to the control system of the core and without experiencing positive reactivity insertion as a result of large core voiding [1]. Drawbacks of the CORAIL design are the relatively high power peaking factor due to the heterogeneous configuration and the need for enriched uranium.

The modeling of the CORAIL assembly is particularly challenging, both because of the presence of degraded plutonium and because of its strong heterogeneities, due to the positioning of MOX pins on the periphery and UO<sub>2</sub> pins in the center of the assembly, which in turn cause a strong flux gradient within the assembly. For this reason a benchmarking effort was initiated between ANL and CEA of France, using both deterministic and Monte Carlo codes [2]. In particular

WIMS8 and MCNP4C where used at ANL, and APOLLO2 and TRIPOLI4 where used at CEA. Initially large discrepancies where found in the evaluated pin power distribution between WIMS8 and APOLLO2. These discrepancies where later largely resolved by using the  $P_{ij} + S_n$  model in APOLLO2 [2].

## 2. PURPOSE OF THE WORK

The purpose of this work is to benchmark the TRITON/NEWT code and associated cross section libraries, part of SCALE 5.1 [3], against results of WIMS8 and APOLLO2, for the CORAIL assembly.

First a static calculation was performed at BOL, mainly comparing  $k_\infty$  and assembly pin power distribution. Afterwards a depletion calculation was performed, and several parameters where compared, including  $k_\infty$ , pin power distribution and most importantly the evolution of various actinides, averaged over the assembly. At this stage a significant disagreement was found in the burnup-dependent concentrations of some of the minor actinides, particularly of  $^{242m}\text{Am}$ . Therefore an effort, presented here, was initiated to understand the reason of this discrepancy. The afore-mentioned discrepancy was traced back to a difference in the branching ratio (BR) of the  $(n,\gamma)$  reaction of  $^{241}\text{Am}$ . After changing the branching ratio in the scale libraries to the values used by WIMS8, the agreement on  $^{242m}\text{Am}$  appeared very satisfactory. Additionally the calculated concentrations of several other minor actinides benefited from this change, particularly of  $^{242}\text{Cm}$ , because it is formed by  $\beta^-$  decay of  $^{242}\text{Am}$ . This demonstrated that the reason of the discrepancy is not due to the cross section libraries, but to the branching ratio used by the codes.

A calculation involving MOX fuel, especially of low isotopic quality such as the CORAIL assembly, should be done with the “general purpose library” of 238 energy groups, distributed with SCALE 5.1. Unfortunately, the memory required by NEWT for this problem is excessive for our computers; therefore it was impossible for us to perform the CORAIL depletion calculation with the 238-groups library. For this reason in the first part of this work we used the standard 44-groups library. In the final part of this work, as SCALE 5.1 became available, we utilized the new capability available in SCALE 5.1 to create an arbitrarily-collapsed cross section library from the 238 master library and created a MOX-specific 44 group library as suggested in [4]. This MOX-specific cross section library has an energy structure refinement around the 1 eV resonance of  $^{240}\text{Pu}$ . It is shown to improve both the calculation of MOX fuel and of standard  $\text{UO}_2$  fuel. In the last part of this work the benchmark is repeated with the new 44-group MOX-specific library, and with both the reference and the modified branching ratios of the  $(n,\gamma)$  reaction of  $^{241}\text{Am}$ .

For the most accurate results, the resolved resonance treatment should be done with CENTRM, a continuous energy transport module. Unfortunately, as of this writing, CENTRM is not recommended by ORNL for reactor calculations at normal operating temperatures because of a yet un-resolved issue with the absorption cross section of  $^{238}\text{U}$ . Therefore the recommended module for un-resolved resonance treatment remains NITAWL, based on the Nordheim method and available with ENDF/B-V based cross sections. Nevertheless we will show some results obtained with CENTRM before the cross section issue was found and made public.

The benchmark in [2] was performed and gives data for both 8 weight percent plutonium and 12 weight percent plutonium. We performed both benchmarks, but for compactness and clarity in this work we only show the results of the 8 weight percent plutonium. The results for the 12 weight percent are similar to the ones shown here for the 8 weight percent plutonium.

### 3. METHODOLOGY

The benchmark specifications [2, 5] include the geometric details shown in Figure 1 and the atomic densities of each of the constituents, shown in Table I for the fuel, Table II and Table III for the coolant densities in cold and hot conditions respectively.

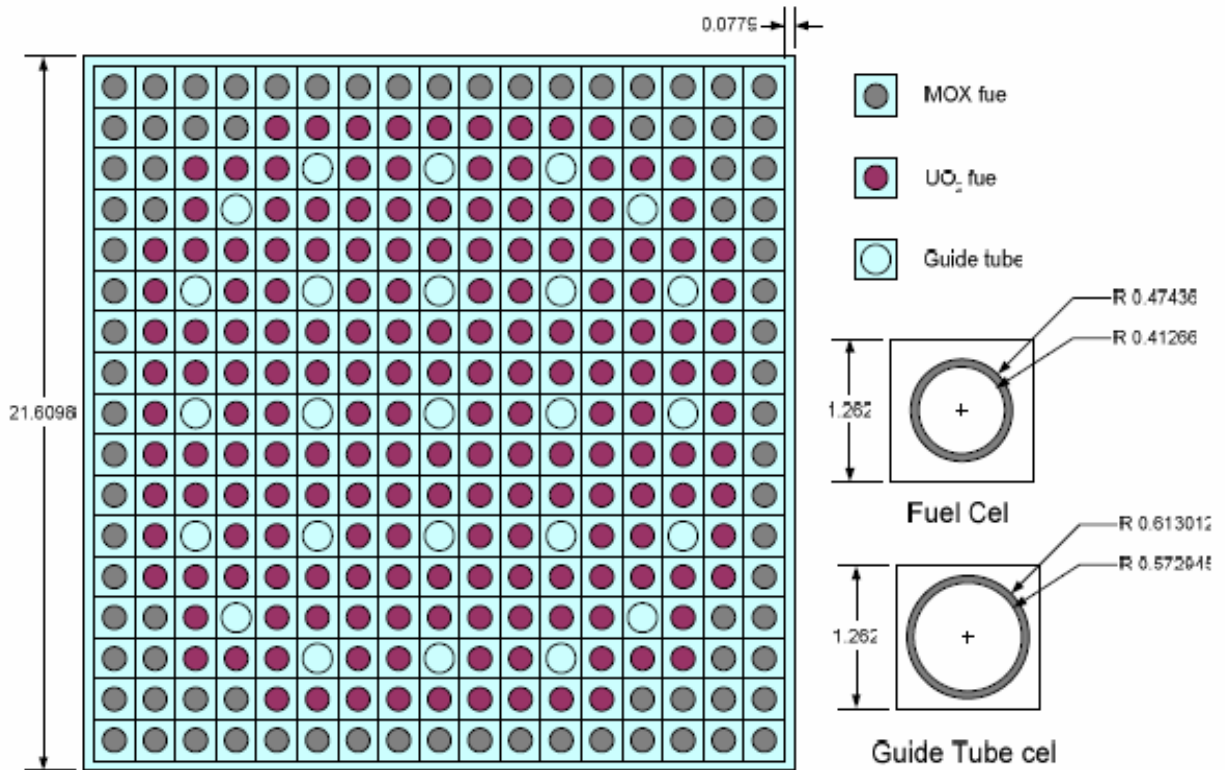


**Figure 1. Geometric configuration of the CORAIL assembly (from [2]).**

The calculations presented in this work are done with the TRITON/NEWT sequence of SCALE 5.0 and 5.1. TRITON is a driver module that uses NEWT to calculate the solution to the transport equation in 2-D, with either 44 or 238 energy groups. The NEWT mesh is 30x30, the order of the  $S_n$  quadrature is 4; the  $P_n$  scattering order is 2 for the water, 1 for the fuel and 0 for the cladding.

The WIMS8 and APOLLO2 calculations used JEF2.2 derived cross section library whereas TRITON for this analysis used ENDF/B-V derived 44 group library; only the BOL static calculation was performed with the 238-groups library. In the release 5.1 of SCALE, ENDF/B-VI was released for use with the continuous energy transport solver CENTRM. No

results are presented in this work with ENDF/B-VI. The multi-group cross sections are evaluated using BONAMI for treating the unresolved resonances with the Bondarenko method, and NITAWL to treat the resolved resonances using the Nordheim method. The depletion is performed by ORIGEN-S.

Figure 2 shows the TRITON/NEWT model of the CORAIL assembly. The model employed simulates explicitly the lower right quadrant of the assembly, with the water gap explicitly evaluated on the side of the MOX pins (this was not the case in both TRIPOLI4 and APOLLO2 in use at CEA). It was explicitly modeled in the WIMS8 and the MCNP4C.

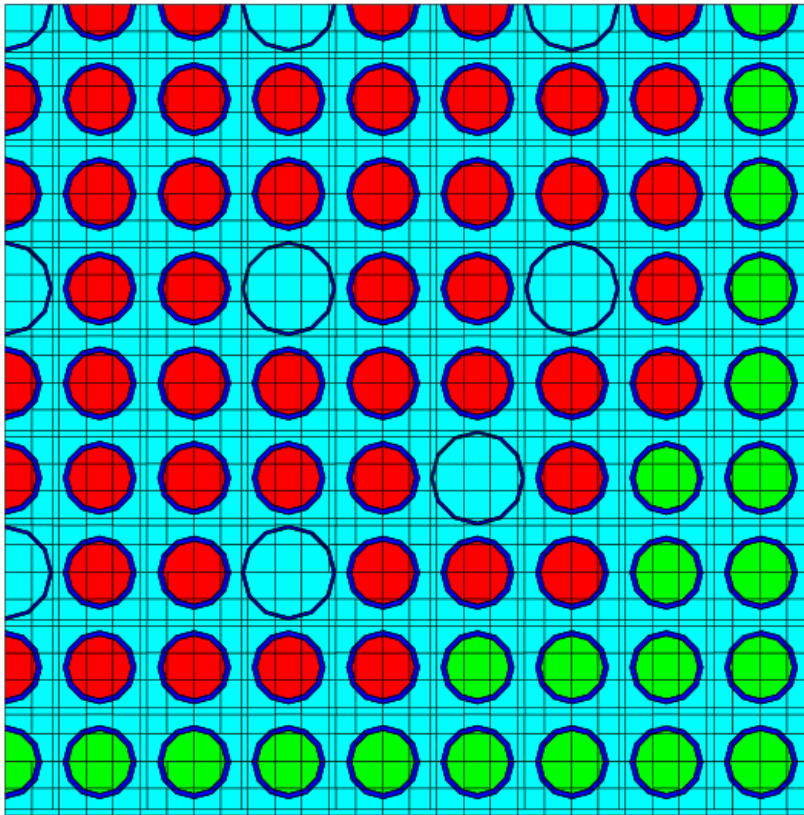


**Figure 2. TRITON model of the CORAIL assembly: bottom-right quarter of the assembly: in red the  $\text{UO}_2$  pins and in green the MOX pins. The water gap is modeled explicitly.**

**Table I. Fuel composition data for CORAIL assembly benchmark**

Assembly Type		CORAIL-Pu <sup>11</sup>	
	Isotope	8% Pu	12% Pu
UO <sub>2</sub> pin	U-235	1.1315E-03	
	U-238	2.1226E-02	
	O-16	4.4716E-02	
MOX pin	U234		
	U235	5.2055E-05	4.9794E-05
	U236		
	U238	2.0508E-02	1.9617E-02
	Np237		
	Pu238	6.9723E-05	1.0459E-04
	Pu239	7.2243E-04	1.0837E-03
	Pu240	5.3327E-04	7.9993E-04
	Pu241	2.1750E-04	3.2627E-04
	Pu242	2.0904E-04	3.1358E-04
	Am241	2.1892E-05	3.2839E-05
	Am242m		
	Am243		
	Cm243		
	Cm244		
	Cm245		
	O	4.4667E-02	4.4655E-02

**Table II. Cold state conditions for CORAIL assembly benchmark**

State	Soluble boron concentration, ppm	Temperature, K (fuel/clad/coolant)	Coolant number density	
			isotope	#/barn.cm
Normal	600	294 / 294 / 294	H <sub>2</sub> O	2.3399E-02
			B-10	4.6584E-06
			B-11	1.8751E-05
Soluble born branch	580	294 / 294 / 294	H <sub>2</sub> O	2.3399E-02
			B-10	4.5019E-06
			B-11	1.8121E-05

**Table III. Hot state conditions for CORAIL assembly benchmark**

State	Soluble boron concentration, ppm	Temperature, K (fuel/clad/coolant)	Coolant number density	
			isotope	#/barn.cm
Normal	600	900 / 630 / 583	H <sub>2</sub> O	2.3399E-02
			B-10	4.6584E-06
			B-11	1.8751E-05
Soluble born branch, 580	580	900 / 630 / 583	H <sub>2</sub> O	2.3399E-02
			B-10	4.5019E-06
			B-11	1.8121E-05
Fuel temperature branch, 850 K	600	850 / 630 / 588	H <sub>2</sub> O	Same as normal state
			B-10	
			B-11	

Due to the lack of individual isotopes of Cr and Fe in the SCALE libraries, the generic material cross sections for both Cr (24000) and Fe (26000) were used, using a number density equal to the total of both nuclei.

## 4. RESULTS

### 4.1. $k_{\infty}$ Evaluation at BOL

The first set of results is an evaluation of  $k_{\infty}$  at BOL. The results of the benchmarks at ANL and CEA are shown in Table IV. To adapt the calculations to the cross sections availability of the Monte Carlo codes (MCNP and TRIPOLI) all the results are at room temperature (294 K). Our results with TRITON are therefore at 294 K as well.

The BOL results from our simulations are shown in Table V together with the difference from MCNP4C with ENDF/B-V (in pcm). In Table V are also shown results for the boron branching at cold temperature, for which no results were provided in [2]. This may be useful for future additional benchmarks.

The agreement with ANL MCNP on the multiplication eigenvalue is very satisfactory (less than 20 pcm and within a standard deviation) when the 44 group cross section library is used, but becomes less satisfactory when the 238 groups library is used. This is likely due to fortuitous compensation of errors.

**Table IV. Benchmark results of the BOL  $k_{\infty}$  from ANL and CEA**

Methodology	Code	Library	$k_{\infty}$	
			8% Pu	12% Pu
Monte-Carlo	MCNP4C	ENDF/B-VI release 2	1.28861 ± 0.00031	1.29541 ± 0.00031
		ENDF/B-VI release 5	1.28906 ± 0.00031	1.29609 ± 0.00031
		ENDF/B-V	1.28937 ± 0.00032	1.29505 ± 0.00029
		JEF-2.2	1.29409 ± 0.00031	1.29992 ± 0.00031
	TRIPOLI 4	JEF-2.2	1.29637 ± 0.00038	1.30187 ± 0.00039
Deterministic transport	WIMS8	JEF-2.2 (6)	1.28645	1.29185
		JEF-2.2 (28)	1.28633	1.29217
		JEF-2.2 (172)	1.28706	1.29263
	APOLLO2	JEF-2.2	1.29649	1.30212

**Table V. Results of the TRITON/NEWT simulations at BOL**

XS library	Condition	BOL $k_{\infty}$	Difference (pcm) from MCNP4C (ANL)
ENDF/B-V 44 groups	Nominal cold	1.289124	-19.0791
ENDF/B-V 238 groups	Nominal cold	1.282912	-500.865
ENDF/B-V 44 groups <sup>(a)</sup>	Nominal cold	1.289145	-17.4504
ENDF/B-V 44 groups	Boron Branch cold	1.290805	N/A

<sup>(a)</sup> Using 38 different zones to evaluate the power distribution and to allow for pin-dependent depletion.

#### 4.2 Pin Power Distribution Evaluation at BOL

In this section are reported the results of the comparison of the pin power distribution at BOL. All the results are reported for the part of the assembly evidenced in Figure 3.

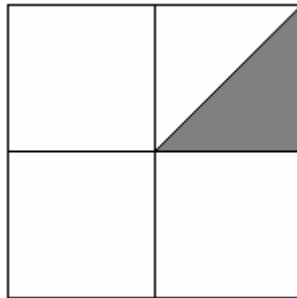


**Figure 3. Fraction of the assembly represented in the present and the following sections**

Table VI shows the normalized pin power distribution and the difference in percent between TRITON with 44 groups and ANL-MCNP4C, with cross sections derived from ENDF/B-VI. The agreement is satisfactory, showing only a maximum discrepancy of 1.72 % and -1.48 %. The agreement is worse between the reported results of ANL and CEA, being as high as 2.8% between TRIPOLI and MCNP4C (using JEF2.2 and ENDF/B-VI respectively).

**Table VI. Normalized pin power distribution at BOL: TRITON results and percent difference from ANL MCNP with ENDF/B-VI. The maximum and minimum discrepancies are 1.72 % and -1.48 % respectively (in red)**

Triton								0.803
% diff	MCNP							0.04%
								0.809
								0.796
								0.82%
								0.64%
								0.767
								0.901
								0.825
								-0.78%
								<b>1.72%</b>
								0.30%
								0.911
								1.024
								0.888
								0.75%
								0.67%
								-0.32%
								1.068
								1.074
								0.992
								0.814
								0.978
								-1.02%
								0.03%
								-0.73%
								0.73%
								1.13%
								1.125
								1.091
								-0.87%
								-0.70%
								0.901
								1.033
								-0.01%
								1.51%
								1.092
								1.145
								1.070
								1.043
								1.029
								0.879
								1.041
								-1.10%
								-0.90%
								-1.05%
								0.17%
								-0.27%
								0.28%
								0.78%
								1.103
								1.101
								1.146
								1.078
								1.044
								1.040
								0.886
								1.056
								-0.70%
								<b>-1.48%</b>
								-0.58%
								-0.58%
								-0.24%
								-0.87%
								0.48%
								0.64%
								1.161
								1.153
								-0.89%
								1.128
								1.099
								-1.11%
								0.37%
								0.932
								1.060
								0.10%
								0.88%

### 4.3. $k_{\infty}$ Evolution with Burnup

Figure 4 shows a comparison of the differences in  $k_{\infty}$  as a function of burnup in pcm, for APOLLO2 and WIMS8 and for a number of cases to be presented in greater detail later in the paper. The difference between APOLLO2 and WIMS8 (blue line) is larger than the difference between TRITON and WIMS8, this despite the fact that both APOLLO2 and WIMS8 use JEF2.2 cross section libraries while TRITON/NEWT uses ENDF/B-V. The difference becomes even smaller when TRITON is compared with the average of WIMS and APOLLO. BR in the caption means “Branching Ratio” and involves changes in the branching ratio of the (n, $\gamma$ ) reaction of  $^{241}\text{Am}$ , for reasons to be explained later in the paper. Changes in this parameter do not alter substantially the calculated eigenvalues. The difference between TRITON and WIMS8 becomes larger than the difference between APOLLO2 and WIMS8 at larger burnups if CENTRM is used to create the multi-group cross sections (brown line with the circle marker).



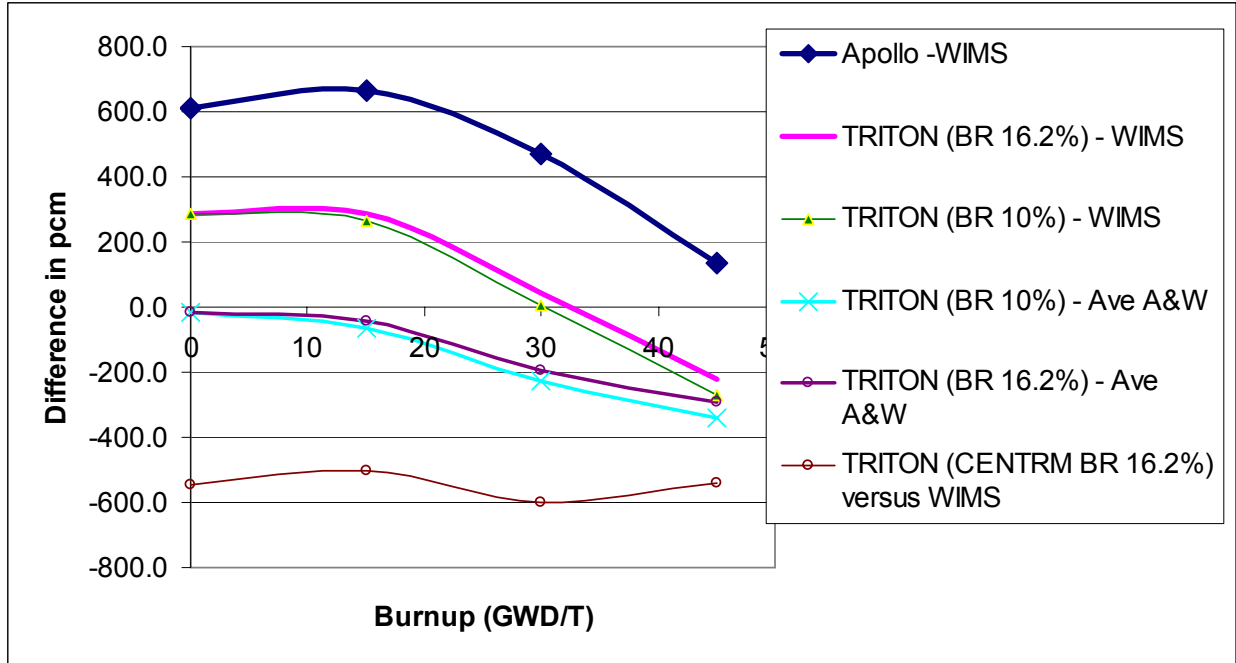


**Figure 4. Evolution with burnup of the differences in the  $k_{\infty}$  (in pcm) between APOLLO and WIMS as compared to TRITON versus WIMS and TRITON versus the average of WIMS and APOLLO. From top to bottom: difference between APOLLO2 and WIMS8, between TRITON and WIMS8 with branching ratios of 16.2% and 10% in the  $(n,\gamma)$  reaction of  $^{241}\text{Am}$ , between the TRITON and the average of WIMS8 and APOLLO2 and between TRITON and WIMS8 when CENTRM is used instead of NITAWL.**

#### 4.4. Pin-Wise Power Distribution; Evolution with Burnup

Pin-wise power distribution data are available in [2] at 0, 15, 30, 45 GWD/T. Table VII and Table VIII show the normalized pin power distribution at 0 GWD/MT (BOL) and at 45 GWD/MT (EOL) respectively. The left sides in both tables show the value of WIMS8 and APOLLO2 and the percent difference between the two, while the right side shows the values of TRITON and the percent difference between both WIMS8 and APOLLO2. The maximum discrepancies (both positive and negative) are evidenced in red. Generally the disagreement is of the same order of magnitude (always less than 3% and mostly less than 2%) as the disagreement between WIMS and APOLLO - even though the latter two use the same cross sections. The disagreement of TRITON is generally larger with APOLLO than with WIMS8, likely reflecting the fact that both WIMS and TRITON model the water gap at the periphery of the assembly explicitly, while APOLLO does not.

**Table VII. Normalized pin power distribution at 0 GWD/MT (BOL). Left side presents the WIMS8 and APOLLO2 results and the percent difference between the two. The maximum and minimum are 1.7 % and -1.5 %. The right side presents the results of TRITON and the percent difference between the WIMS8 and the APOLLO2 results: the maximum and minimum are 1.42 % and -1.65 % with WIMS8 and APOLLO2 respectively**

WIMS								0.811						
Apollo								0.799						
% diff								-1.5						
							0.825	0.803						
							0.839	0.805						
							1.7	0.2						
							0.747	0.927	0.839					
							0.747	0.939	0.836					
							0	1.3	-0.4					
							0.876	1.062	0.911					
							0.876	1.078	0.904					
							0	1.5	-0.8					
							1.066	1.045	0.962	0.793	1.014			
							1.067	1.047	0.963	0.796	1.007			
							0.1	0.2	0.1	0.4	-0.7			
							1.104	1.064		0.867	1.081			
							1.103	1.066		0.871	1.068			
							-0.1	0.2		0.5	-1.2			
							1.104	1.13	1.075	1.038	1.004	0.861	1.098	
							1.101	1.127	1.074	1.038	1.006	0.865	1.088	
							-0.3	-0.3	-0.1	0	0.2	0.5	-0.9	
							1.117	1.111	1.133	1.081	1.044	1.012	0.869	1.111
							1.11	1.106	1.131	1.077	1.042	1.013	0.873	1.099
							-0.6	-0.5	-0.2	-0.4	-0.2	0.1	0.5	-1.1
							1.152	1.147		1.116	1.076		0.898	1.12
							1.149	1.146		1.116	1.08		0.904	1.108
							-0.3	-0.1		0	0.4		0.7	-1.1

	Triton													0.807						
% diff	WIMS													-0.47						
% diff	Apollo													1.02						
													0.825	0.804						
													0.02	0.18						
													-1.65	-0.06						
													0.745	0.934	0.841					
													-0.30	0.76	0.18					
													-0.30	-0.53	0.54					
													0.878	1.077	0.913					
													0.26	1.40	0.26					
													0.26	-0.11	1.04					
													1.052	1.044	0.958	0.791	1.020			
													-1.28	-0.08	-0.39	-0.20	0.55			
													-1.37	-0.27	-0.50	-0.58	1.25			
													1.106	1.068		0.871	1.083			
													0.20	0.40		0.45	0.20			
													0.29	0.22		-0.01	1.42			
													1.093	1.132	1.066	1.034	1.004	0.860	1.095	
													-0.98	0.16	-0.87	-0.38	0.05	-0.07	-0.28	
													-0.71	0.43	-0.78	-0.38	-0.15	-0.53	0.64	
													1.107	1.104	1.136	1.075	1.038	1.016	0.868	1.112
													-0.90	-0.66	0.22	-0.58	-0.61	0.39	-0.06	0.10
													-0.27	-0.21	0.40	-0.21	-0.42	0.29	-0.52	1.20
													1.153	1.144		1.114	1.081		0.904	1.117
													0.08	-0.29		-0.16	0.49		0.68	-0.29
													0.34	-0.20		-0.16	0.12		0.02	0.79



**Table IX. Percent difference in the assembly-average concentrations in TRITON as compared to WIMS for the case of NITAWL and 16.2% <sup>241</sup>Am branching ratio**

	APOLLO2 versus WIMS8			TRITON versus WIMS8		
	15 GWD/T	30 GWD/T	45 GWD/T	15 GWD/T	30 GWD/T	45 GWD/T
U-234	-0.1%	-1.0%	-1.4%	-2.5%	-8.6%	-4.0%
U-235	-0.1%	-0.1%	-0.3%	-2.1%	1.0%	-7.8%
U-236	0.2%	-1.0%	-2.4%	7.8%	2.0%	4.8%
U-238	0.0%	0.0%	0.0%	0.0%	0.1%	-0.1%
Pu-238	-0.3%	0.2%	1.6%	-0.5%	-1.5%	0.4%
Pu-239	-2.0%	-3.7%	-5.5%	0.5%	-2.2%	-4.1%
Pu-240	0.1%	-0.2%	-0.8%	-0.5%	-1.1%	-2.7%
Pu-241	-0.5%	-1.4%	-2.5%	1.1%	-1.1%	-1.5%
Pu-242	-0.4%	-0.5%	-0.7%	1.8%	1.8%	5.0%
Am-241	-0.9%	-2.0%	-3.4%	2.3%	1.5%	1.1%
Am-242m	13.2%	11.0%	9.0%	42.4%	61.2%	61.4%
Am-243	5.5%	4.9%	4.3%	4.0%	6.0%	16.7%
Cm-242	1.1%	0.5%	-0.3%	-8.6%	-10.1%	-6.9%
Cm-243	1.9%	0.8%	-0.3%	18.2%	8.1%	14.0%
Cm-244	6.2%	5.8%	5.1%	-7.3%	-10.8%	5.8%
Cm-245	5.5%	4.8%	2.9%	-26.6%	-35.4%	-23.2%

**Table X. Percent difference in the assembly-average concentrations in TRITON as compared to WIMS for the case of CENTRM and 16.2% <sup>241</sup>Am branching ratio**

	TRITON (nitawl 44) versus WIMS8			TRITON (centrm 44) versus WIMS8		
	15 GWD/T	30 GWD/T	45 GWD/T	15 GWD/T	30 GWD/T	45 GWD/T
U-234	-2.5%	-8.6%	-4.0%	-2.5%	-8.6%	-3.8%
U-235	-2.1%	1.0%	-7.8%	-1.8%	1.9%	-5.5%
U-236	7.8%	2.0%	4.8%	7.1%	1.3%	4.0%
U-238	0.0%	0.1%	-0.1%	-0.1%	0.0%	-0.2%
Pu-238	-0.5%	-1.5%	0.4%	-0.5%	-1.4%	0.5%
Pu-239	0.5%	-2.2%	-4.1%	2.1%	0.7%	0.4%
Pu-240	-0.5%	-1.1%	-2.7%	0.2%	0.4%	-0.3%
Pu-241	1.1%	-1.1%	-1.5%	1.6%	0.2%	1.3%
Pu-242	1.8%	1.8%	5.0%	0.8%	0.0%	2.2%
Am-241	2.3%	1.5%	1.1%	2.3%	2.3%	4.1%
Am-242m	42.4%	61.2%	61.4%	44.3%	64.3%	67.9%
Am-243	4.0%	6.0%	16.7%	7.2%	7.2%	15.6%
Cm-242	-8.6%	-10.1%	-6.9%	-8.7%	-10.7%	-7.6%
Cm-243	18.2%	8.1%	14.0%	17.6%	6.8%	12.3%
Cm-244	-7.3%	-10.8%	5.8%	8.4%	1.4%	15.4%
Cm-245	-26.6%	-35.4%	-23.2%	7.6%	-5.4%	11.5%

#### 4.6. Branching Ratio

The large discrepancy observed in  $^{242m}\text{Am}$  prompted us to investigate the effect of the branching ratio of the  $(n,\gamma)$  reaction of  $^{241}\text{Am}$ . The branching ratio is energy dependent, therefore it needs to be evaluated by spectrum-weighting the energy-dependent branching ratio using Equation 1 (where  $f_{\gamma 1}(E)$  is the energy dependent branching ratio).

$$\bar{f}_{\gamma 1} = \frac{\int_0^{\infty} f_{\gamma 1}(E) \sigma_c(E) \phi(E) dE}{\int_0^{\infty} \sigma_c(E) \phi(E) dE} \quad (1)$$

We obtained from [5] the data in Figure 5, showing the branching ratio of the  $(n,\gamma)$  reaction of  $^{241}\text{Am}$  to generate  $^{242}\text{Am}$  (and  $^{242m}\text{Am}$ ) as a function of energy. All the most recent nuclear data file show a good agreement in the thermal region and, with the exception of JENDL-3.3, a similar behavior also in the epithermal region.

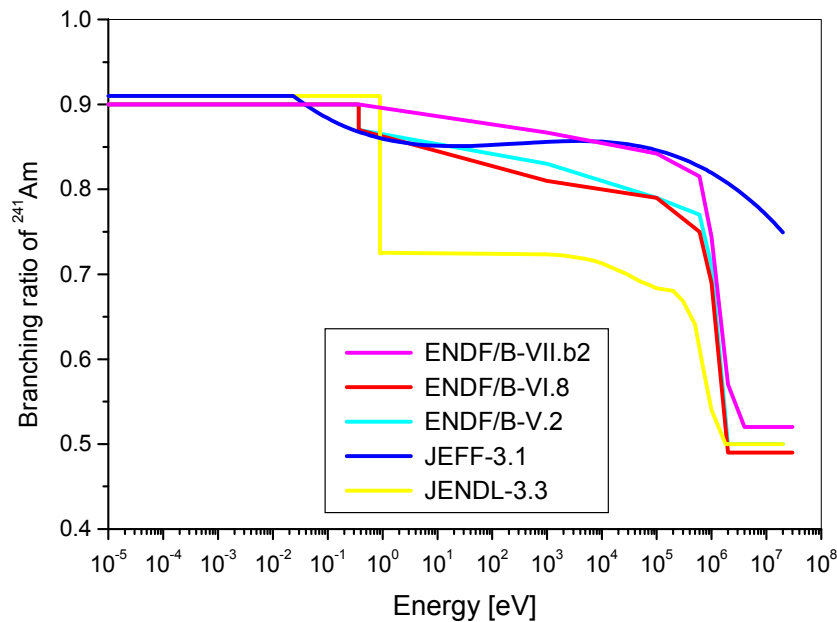


Figure 5. Branching ratio of  $^{241}\text{Am}$   $(n,\gamma)$  reaction.

The default SCALE 5.1 libraries of the depletion module ORIGEN-S have a branching ratio of 16.2% for the creation of  $^{242m}\text{Am}$  from the  $(n,\gamma)$  reaction of  $^{241}\text{Am}$ .

To estimate how accurate this number is with respect to the more recent evaluations, we performed a spectrum weighting on the typical spectra for few representative fuel types.

Starting from the energy-dependence of the branching ratio shown in Figure 5 for the ENDF/B-VI (red line), we weighted it over the fluxes of a typical PWR with  $\text{UO}_2$  5% enriched and with MOX. Additionally we integrated over the CORAIL average fuel spectrum and over

the average spectrum of PUZH fuel<sup>1</sup>, which is softer than that MOX because of the presence of hydrogen in the fuel itself.

As an example we will consider the average spectrum of the CORAIL assembly. Figure 6 shows the average spectrum of the CORAIL assembly inside the fuel. The (n,γ) cross section of <sup>241</sup>Am is plotted in Figure 7. The weighting of this cross section over the flux of the CORAIL is shown in Figure 8, in thick blue the numerator and in light pink the denominator. Most of the reactions occur in the thermal region up to 10 eV, with some occurring in the epithermal region and almost none in the fast region.

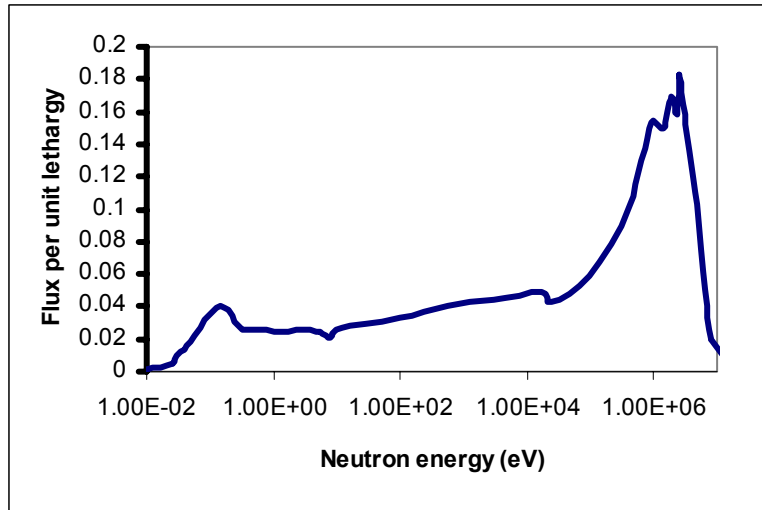


Figure 6. Average fuel neutron flux normalized per unit lethargy of CORAIL assembly.

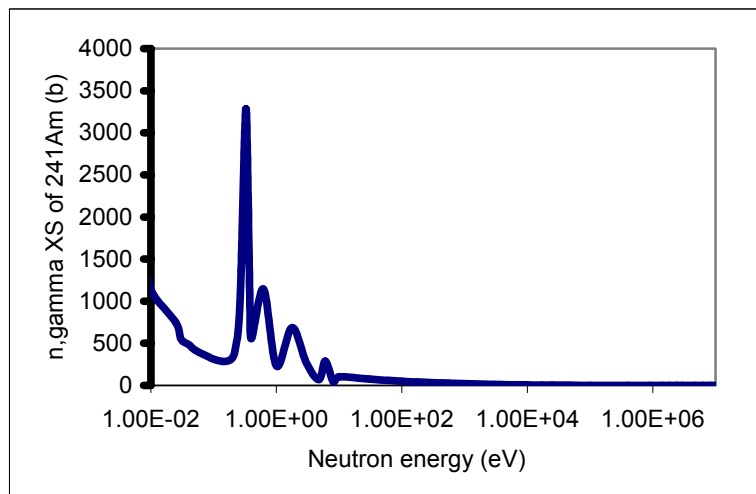
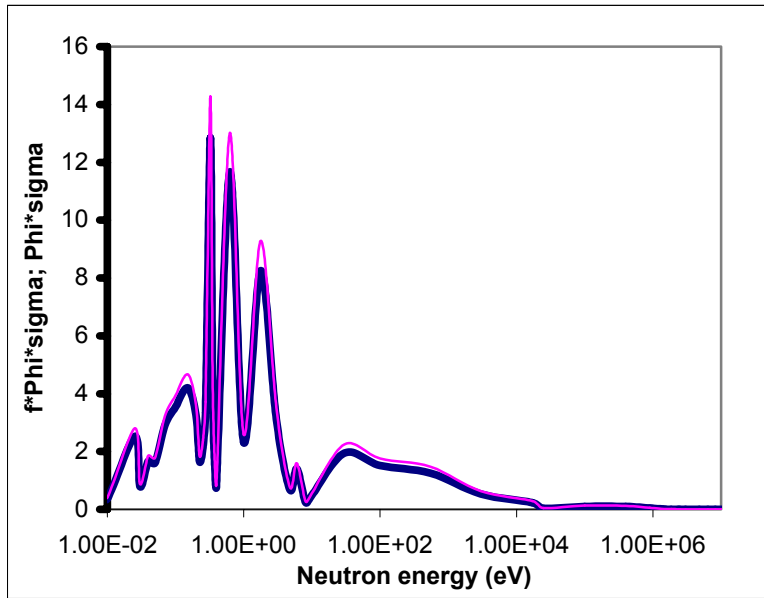


Figure 7. (n,γ) cross section of <sup>241</sup>Am.

<sup>1</sup> PUZH is an acronym for a hydride fuel of the type U-PuH<sub>2</sub>-ZrH<sub>1.6</sub>, which has been studying extensively at UCB as an alternative for the disposition of plutonium in PWR.



**Figure 8. Product of (n, $\gamma$ ) XS of  $^{241}\text{Am}$  and neutron flux: the ratio of the areas under the two curves is the evaluated branching ratio of  $^{242\text{m}}\text{Am}$ .**

The resulting evaluated branching ratios are shown in Table XI for the previously mentioned fuel types. All the resulting branching ratios are of the order of 10% to 11%, making the SCALE 5.1 default value of 16.2% clearly inadequate. Recently presented measurements at the CEA labs of Saclay and Cadarache further confirmed these results, measuring a branching ratio of  $10.5\% \pm 0.1\%$  at 0.025 eV [6].

**Table XI. Resulting evaluated branching ratios for different typical fuel types spectra**

	PWR	MOX	PUZH	CORAIL
BR $^{242}\text{Am}$	0.884	0.893	0.889	0.893
BR $^{242\text{m}}\text{Am}$	0.116	0.107	0.111	0.107

#### 4.7. Re-evaluation of the Benchmark's Results with the New Branching Ratio

WIMS8 in use at ANL uses a branching ratio of 10%, while APOLLO2 uses 11.5% for (n, $\gamma$ ) capture reaction of  $^{241}\text{Am}$ . To test the importance of the branching ratio on the observed discrepancy of  $^{242\text{m}}\text{Am}$ , we changed the branching ratio in the scale binary libraries to 10%, and re-performed the benchmark calculation.

The branching ratio in the ORIGEN-S binary library can be changed by, first, modifying the value of interest in the ASCII ORIGEN-S library, which contains the default three-group cross sections and branching ratios. Afterwards it is required to re-construct the binary library

which is used and updated by the transport/depletion modules (like SAS2H and TRITON). This second step requires the execution of a “stand alone” BONAMI module, followed by SAS2H to create light water reactor specific cross sections. Finally it is necessary to transfer the resulting binary library into the working directory of SCALE, and to re-run BONAMI and SAS2H to finalize the library creation. All this was performed successfully: the branching ratio contained in the binary library was verified by a confirmatory run of TRITON with very short time steps.

Table XII compares the calculated nuclei evolutions using the new libraries with a 10% branching ratio (on the right side) to the nuclei evolution in case of 16.2% branching ratio (on the left side). The disagreement on the  $^{242m}\text{Am}$  evolution virtually disappears, confirming our assumption that the discrepancy found initially was mainly due to the difference in the branching ratio. The other differences are roughly similar, with the exception of  $^{242}\text{Cm}$ , which is formed mainly by  $\beta^-$  decay of  $^{242}\text{Am}$ . Large discrepancies in the number densities of heavier actinides, especially the curium isotopes are well known and documented in the literature: for example the reported uncertainties in the number densities of curium isotopes in the OECD-proposed benchmark A for Pu recycling in PWR, [7] are: 17%, 26%, 11% and 19% for respectively  $^{242}\text{Cm}$ ,  $^{243}\text{Cm}$ ,  $^{244}\text{Cm}$ ,  $^{245}\text{Cm}$ . Except for  $^{245}\text{Cm}$  these values exceed the discrepancies found between TRITON/NEWT and WIMS8. Additionally, in [7] most of the calculations were done with JEF, few with JENDL and none with ENDF (CASMO-3 was withdrawn).

**Table XII. Percent difference in the assembly-average concentrations in TRITON as compared to WIMS for the case of NITAWL with 10%  $^{241}\text{Am}$  branching ratio**

	TRITON BR 16.2% versus WIMS8			TRITON BR 10% BR versus WIMS8		
	15 GWD/T	30 GWD/T	45 GWD/T	15 GWD/T	30 GWD/T	45 GWD/T
<b>U-234</b>	-2.50%	-8.60%	-4.00%	-5.40%	-5.70%	-5.70%
<b>U-235</b>	-2.10%	1.00%	-7.80%	-0.70%	-1.80%	-2.90%
<b>U-236</b>	7.80%	2.00%	4.80%	4.60%	4.20%	3.20%
<b>U-238</b>	0.00%	0.10%	-0.10%	0.00%	0.00%	0.00%
<b>Pu-238</b>	-0.50%	-1.50%	0.40%	-0.10%	0.00%	0.90%
<b>Pu-239</b>	0.50%	-2.20%	-4.10%	0.50%	-2.60%	-3.20%
<b>Pu-240</b>	-0.50%	-1.10%	-2.70%	-0.60%	-1.30%	-2.20%
<b>Pu-241</b>	1.10%	-1.10%	-1.50%	0.60%	-0.50%	-1.50%
<b>Pu-242</b>	1.80%	1.80%	5.00%	1.50%	2.60%	3.80%
<b>Am-241</b>	2.30%	1.50%	1.10%	2.10%	1.60%	1.60%
<b>Am-242m</b>	42.40%	61.20%	61.40%	-13.10%	-0.30%	0.30%
<b>Am-243</b>	4.00%	6.00%	16.70%	0.20%	9.10%	12.30%
<b>Cm-242</b>	-8.60%	-10.10%	-6.90%	-3.90%	-1.90%	-1.70%
<b>Cm-243</b>	18.20%	8.10%	14.00%	20.10%	20.80%	18.40%
<b>Cm-244</b>	-7.30%	-10.80%	5.80%	-13.90%	-5.00%	-1.50%
<b>Cm-245</b>	-26.60%	-35.40%	-23.20%	-34.20%	-29.40%	-29.50%



#### 4.8. Change of the 44 group cross section

The general purpose multi-group cross section distributed with the SCALE 5.1 code system is a 238 group library based on ENDF/B-V. Extensive benchmarks for MOX fuel systems [4, 9] have shown that this library is capable of adequate representation of plutonium bearing fuels with highly depleted plutonium.

Unfortunately, when multiple mixtures have to be depleted independently and with high accuracy - our CORAIL assembly model follows 240 nuclides in 39 different fuel mixtures - the memory requirement for NEWT becomes excessive if the 238 group library is used. The standard 44 group cross section library used in the CORAIL calculations described above was obtained by collapsing the multi-purpose 238 group library using a spectrum corresponding to a reference 3.3 % enriched LWR fuel assembly. This library was found [4] inadequate to model MOX fuel with plutonium of low isotopic quality. A modified 44 group structure was proposed [4] with the intent of better capturing the 1 eV resonance structure of  $^{240}\text{Pu}$ . Conforming to the notation introduced in [4] we will call the standard 44 group library as 44-UOX and the one proposed specifically for MOX fuels as 44-MOX. Additionally we will refer to the 238 group library as 238-REF. The basic energy group structure of 44-MOX is the same as of the 44-UOX with the following exceptions: the energy groups between 0.65 eV and 1 eV (group 25) and between 1 eV and 1.77 eV (group 24) have been expanded into 4 energy groups (0.65 to 0.9 eV, 0.9 to 1.07 eV, 1.07 to 1.25 eV and 1.25 to 1.77 eV). To maintain the total number of groups at 44, 4 groups in the fast region (3 MeV to 20 MeV) were condensed into 2 groups: between 3 and 6.43 MeV and between 6.43 and 20 MeV. Extensive testing was conducted in [4], where the 44-MOX library was found to produce better  $k_{\infty}$  and neutron flux values for low-quality plutonium than the 44-UOX.

Version 5.1 of the SCALE code system provides the capability to build user designed libraries, condensed from a higher resolution library such as the multi-purpose 238-REF. In this section are shown the results of the CORAIL benchmark performed with the 44-MOX library we generated from 238-REF using the group structure suggested in [4] and using, for the weighting spectrum, the BOL spectrum calculated for a stand-alone MOX unit cell of a composition and geometry found at the periphery of the CORAIL assembly. .

Figure 9 shows the  $k_{\infty}$  evolution with burnup of the reference peripheral MOX fuel pin using the three libraries: 44-MOX and 44-UOX and 238-REF. The 44-UOX library tends to over-predict  $k_{\infty}$  as compared to the 238-REF for large burnups. Figure 10 shows the percent difference of the two 44-groups libraries versus the 238-groups library. It is observed that the 44-MOX library reduces substantially the discrepancy.

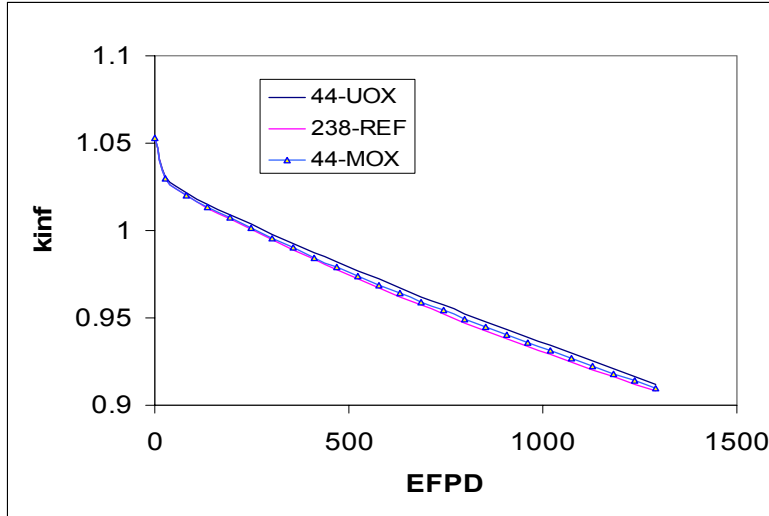


**Figure 9.**  $k_{\infty}$  evolution with burnup for the representative MOX CORAIL periphery pin cell, calculated using the 238-groups, 44-MOX and 44-UOX libraries.

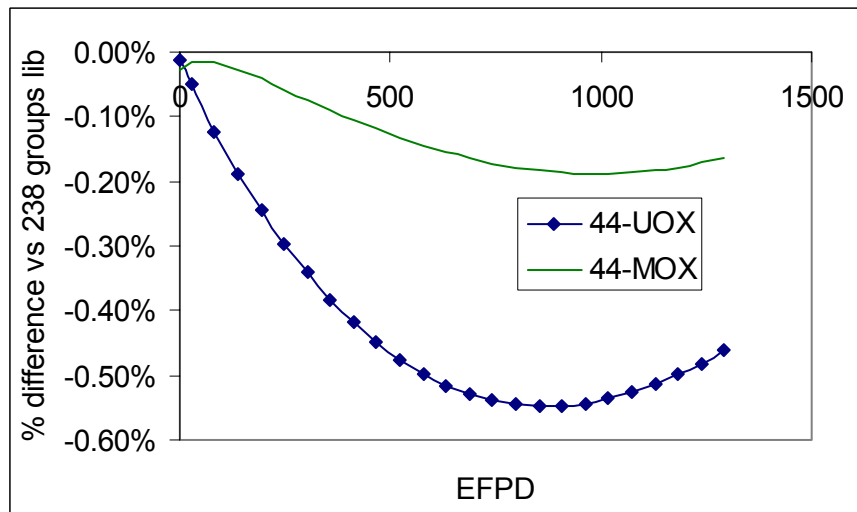


**Figure 10.** Percent difference of the two 44 group libraries versus the 238-groups library.

The reason for the smaller discrepancy of 44-MOX library in the evolution of  $k_{\infty}$  as compared to the 44-UOX library can be understood by comparing, in Figure 11, 12 and 13, the multi-group macroscopic total cross sections (in 1/cm) for the most important nuclei in MOX. In particular it is important to observe the representation of the 1 eV resonance of  $^{240}\text{Pu}$ . Figure 11 shows the “theoretical” shape of the resonance, and Figures 12 and 13 show how this (and other) cross sections are represented in the two 44-UOX and 44-MOX libraries, respectively. The 1 eV resonance of  $^{240}\text{Pu}$  appears better represented in the 44-MOX library as compared to the 44-UOX library.

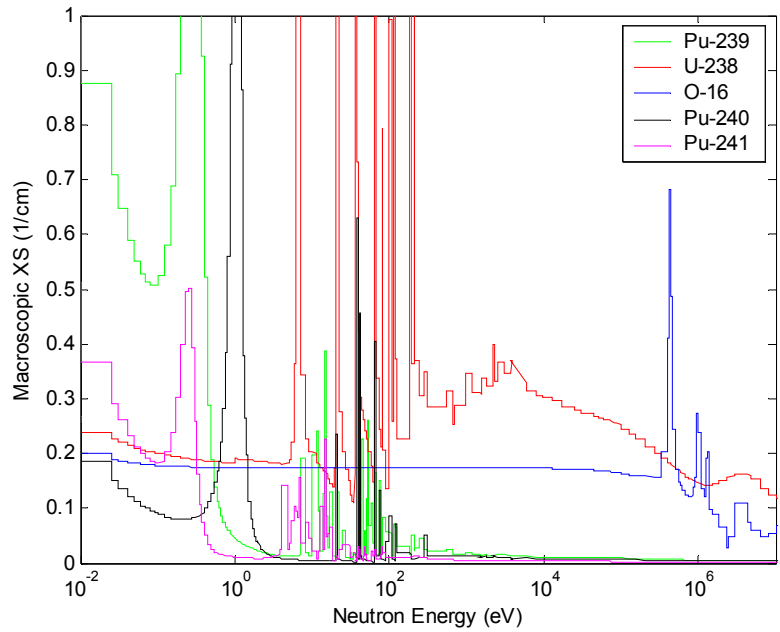


**Figure 11. Macroscopic total cross section (1/cm) for the most important nuclei in MOX (238-REF library).**

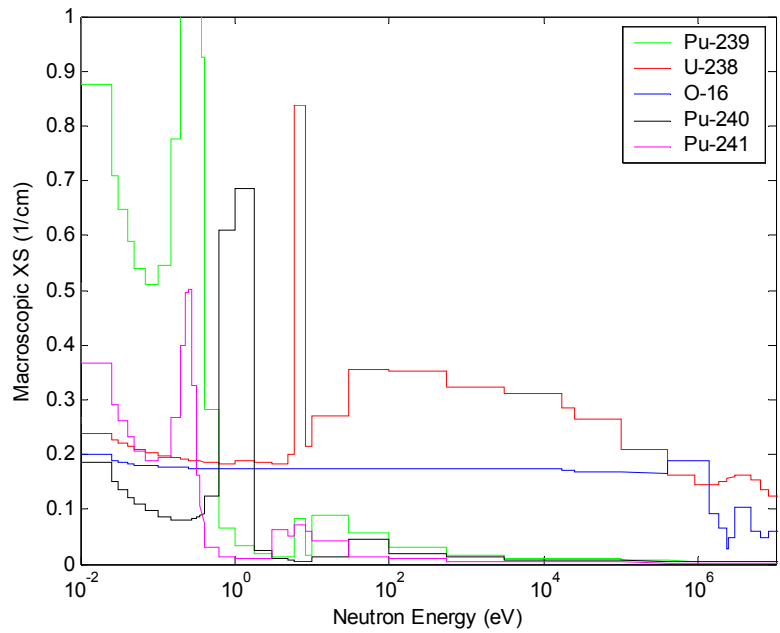


**Figure 12. Macroscopic total cross section (1/cm) for the most important nuclei in MOX (44-UOX library).**

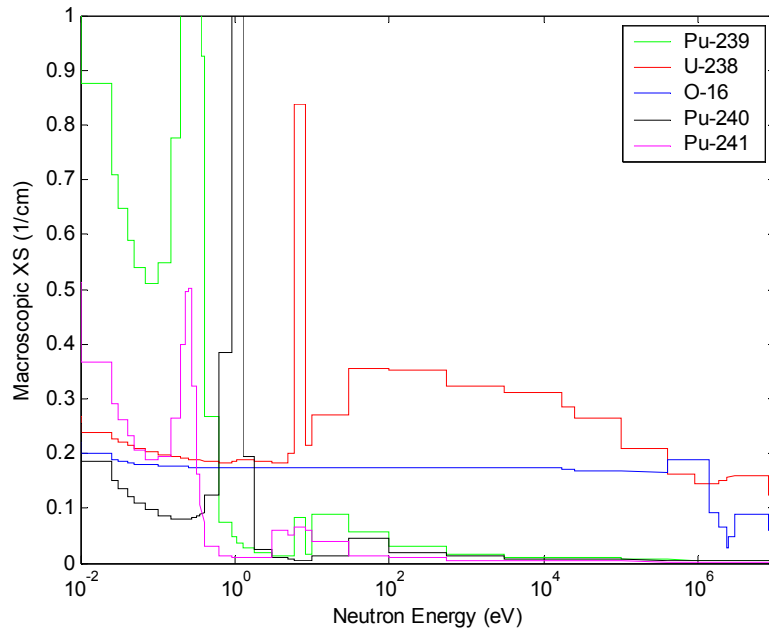


**Figure 13. Macroscopic total cross section (1/cm) for the most important nuclei in MOX (44-MOX library).**

The effect of the different representation of the 1 eV  $^{240}\text{Pu}$  resonance on the neutron spectrum are shown in Figures 14 and 15 for, respectively, the entire spectrum and the thermal energy range. The green line represents the reference spectrum calculated using the 238-REF. The red line represents the 44-UOX spectrum and the blue line the 44-MOX spectrum. The improved representation of the 1 eV resonance of  $^{240}\text{Pu}$  can be appreciated by looking at Figure 15, where the dip in the flux created by the  $^{240}\text{Pu}$  low-lying resonance appears in the 44-MOX library and does not appear at all in the 44-UOX library.

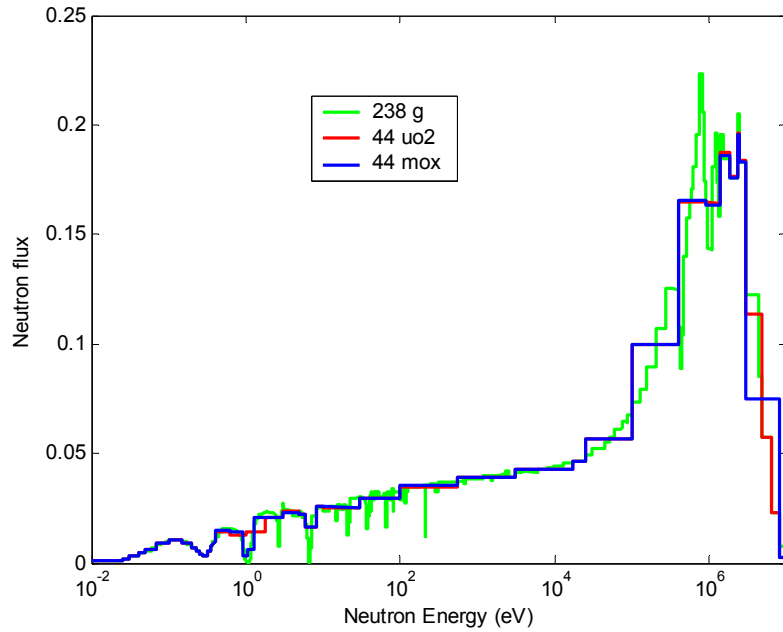


**Figure 14. Neutron flux in the MOX representative pin cell, as evaluated using 238 groups (green line), 44-UOX (red line) and 44-MOX (blue line).**

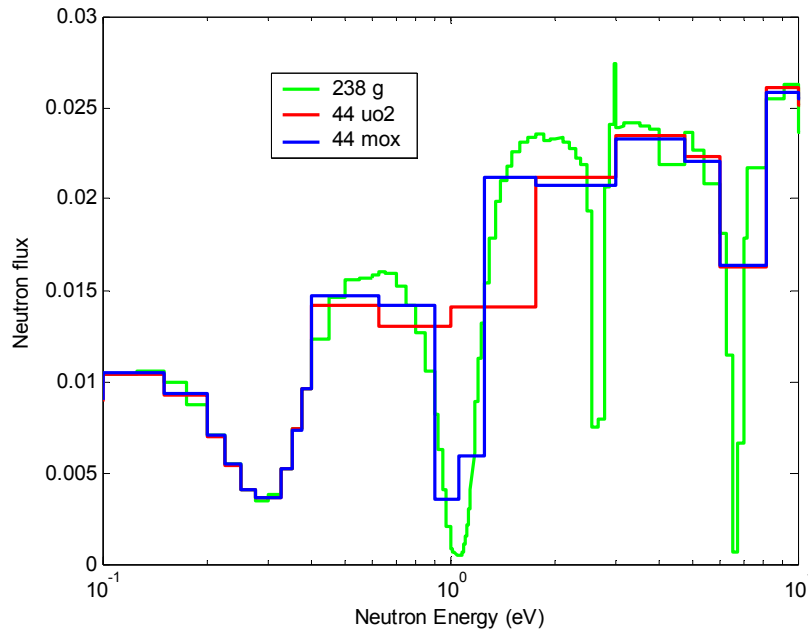


**Figure 15. Neutron flux in the MOX representative pin cell, as evaluated using 238 groups (green line), 44-UOX (red line) and 44-MOX (blue line); thermal spectrum.**

Next consider the ability of the 44-MOX library to predict the performance of UO<sub>2</sub> containing unit cells, since the central part of the CORAIL assembly is made of such cells. For this purpose

the MOX study was repeated using a 5 % enriched representative  $UO_2$  fueled unit cell. As can be deduced from Figures 16 and 17, the results calculated for this unit cell type using the 44-MOX library were found in better agreement with the 238-REF results than the results calculated using the 44-UOX library.

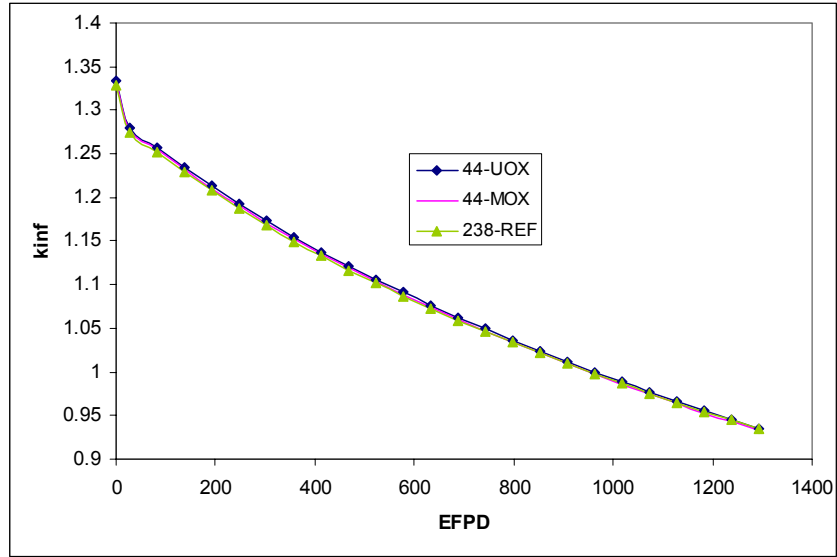


**Figure 16.  $k_{\infty}$  evolution with burnup for a CORAIL reference central  $UO_2$  pin cell 5% enriched.**

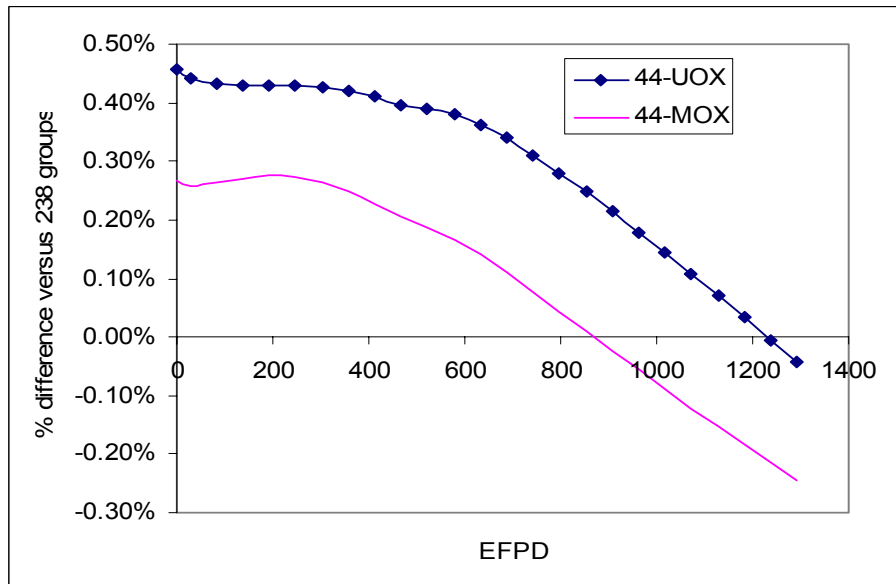


**Figure 17. Percent difference in  $k_{\infty}$  as a function of burnup for a CORAIL reference central  $UO_2$  pin cell 5%enriched.**

The reason for the smaller discrepancy of 44-MOX library in the evolution of  $k_{\infty}$  as compared to the 44-UOX library can be understood by comparing, in Figure 18, 19 and 20, the multi-group representation of the macroscopic total cross sections for the most important nuclei in  $\text{UO}_2$  at BOL. Of particular relevance is the representation of the small resonance of  $^{235}\text{U}$  at 1 eV, green line in Figure 18. Figures 19 and 20 show how this small resonance is observable in the 44-MOX libraries representation (Figure 20), but is not visible in the 44-UOX representation (Figure 19). This has an effect on the calculated multi-group fluxes Shown in Figures 21 and 22.

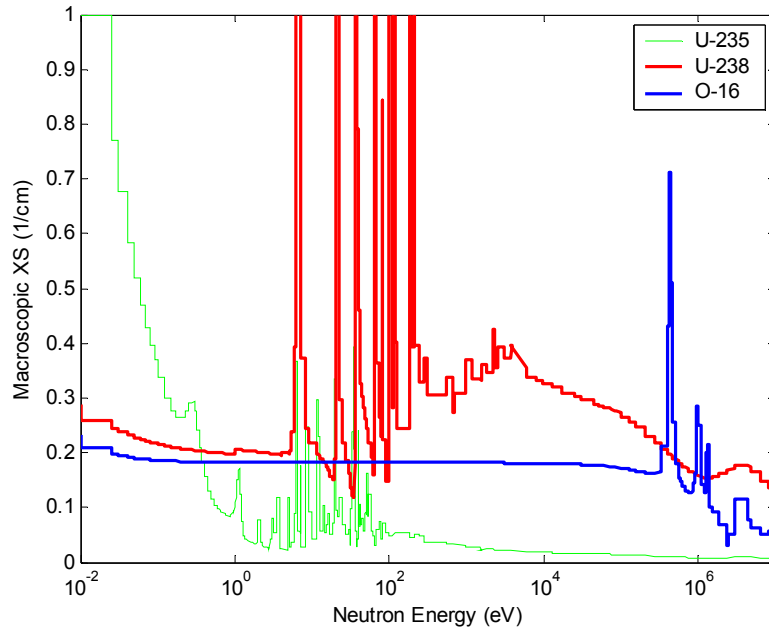


**Figure 18. Macroscopic total cross section (1/cm) for the most important nuclei in  $\text{UO}_2$  (238-REF library).**

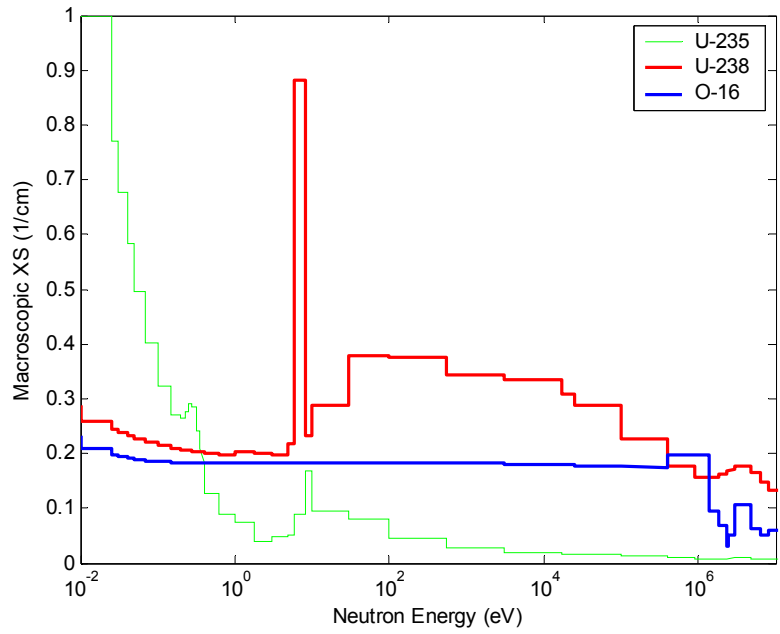


**Figure 19. Macroscopic total cross section (1/cm) for the most important nuclei in UO<sub>2</sub> (44-UOX library).**

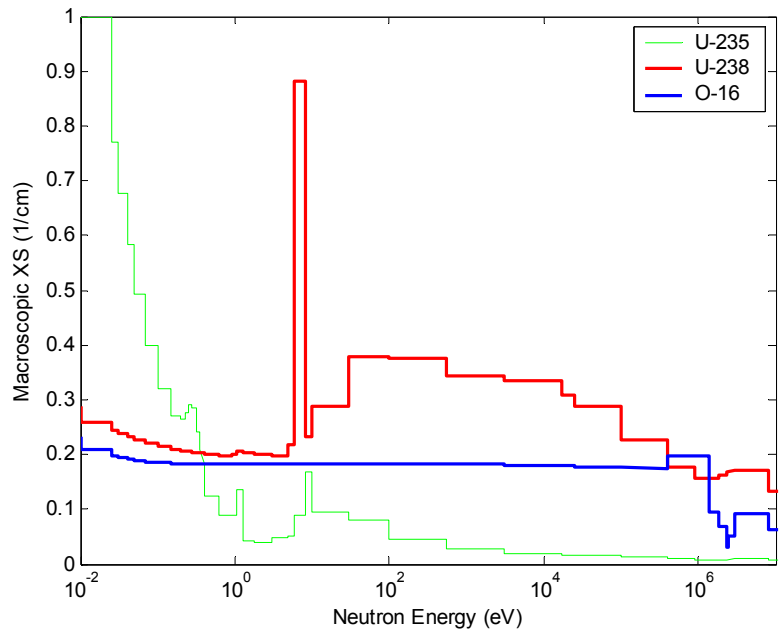


**Figure 20. Macroscopic total cross section (1/cm) for the most important nuclei in UO<sub>2</sub> (44-MOX library).**



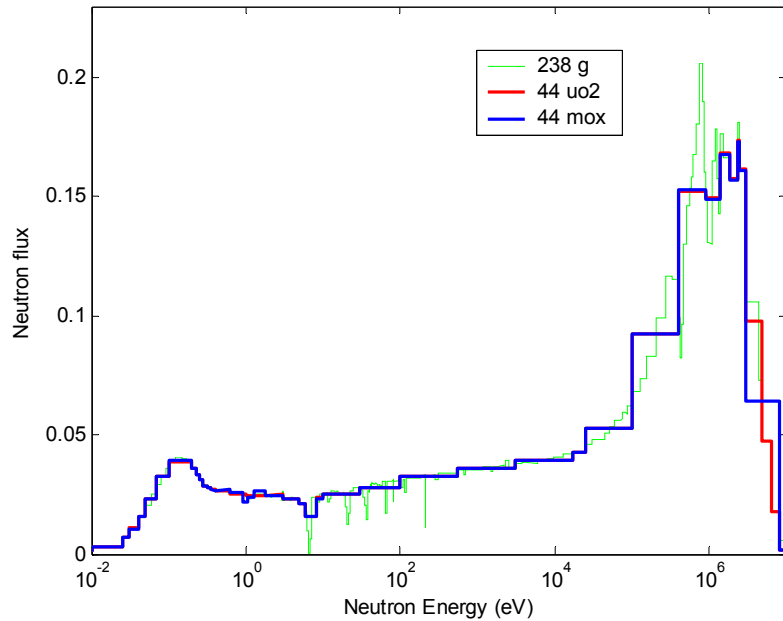


**Figure 21. Neutron flux in the  $\text{UO}_2$  representative pin cell, as evaluated using 238-REF (green line), 44-UOX (red line) and 44-MOX (blue line).**

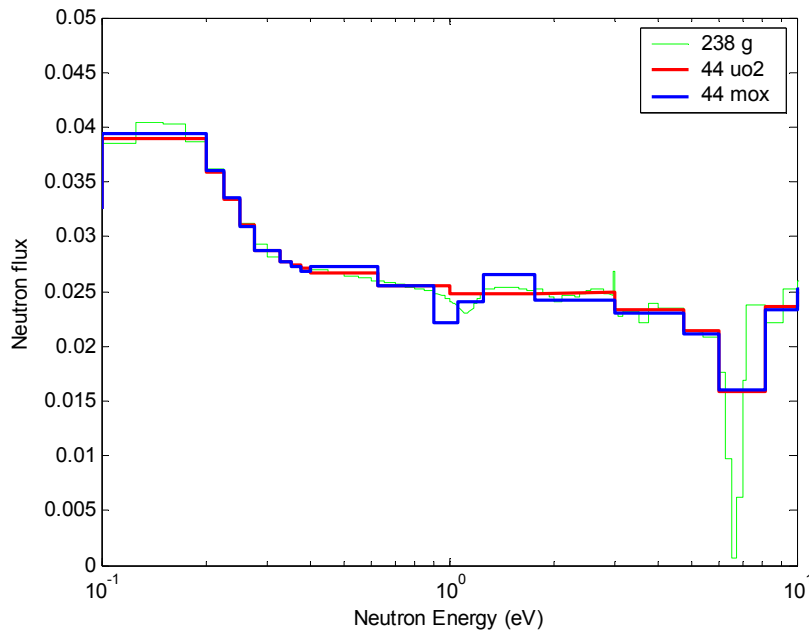


**Figure 22. Neutron flux in the  $\text{UO}_2$  representative pin cell, as evaluated using 238-REF (green line), 44-UOX (red line) and 44-MOX (blue line); enlargement of the thermal region.**

After having shown that the 44-MOX library offers better agreement than the 44-UOX library for both MOX and  $\text{UO}_2$  fuels, we used the 44-MOX library to re-perform the CORAIL assembly benchmark.

Figure 23 shows the difference in pcm between the  $k_{\infty}$  evolution (similar to Figure 4) between TRITON and the benchmark averages. As compared to Figure 4, one more line has been added, showing the discrepancy between the 238-REF and the 44-MOX libraries with a 10% branching ratio for the  $(n,\gamma)$  reaction of  $^{241}\text{Am}$ . The agreement with the average of WIMS8 and APOLLO2 appears similar to the case with the 44-UOX library.

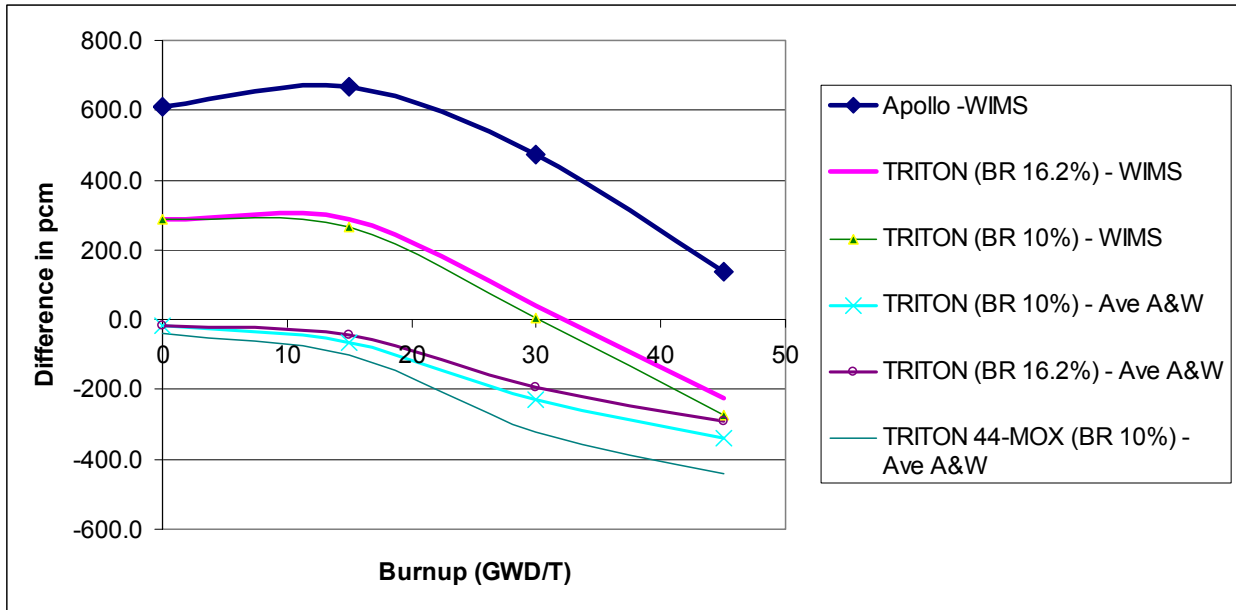


**Figure 23. Evolution with burnup of the differences in the  $k_{\infty}$  (in pcm) between APOLLO2 and WIMS8 as compared to TRITON versus WIMS8 and TRITON versus the average of WIMS8 and APOLLO2. As compared to Figure 4 the percent difference between the average of APOLLO2 and WIMS8 and the TRITON results with the 44-MOX library have been added, with a 10% branching ratio for the  $(n,\gamma)$  reaction of  $^{241}\text{Am}$ .**

Table XIII shows, on the right, the percent difference in the assembly average actinides concentrations between TRITON with the 44-MOX library and WIMS8. These values are to be compared with the ones obtained using the 44-UOX library, shown on the left. The resolved resonance treatment is performed by NITAWL.

Most of the nuclei show a reduced discrepancy when 44-MOX libraries are used, with a substantial improvement particularly in the evolution with burnup of  $^{243}\text{Am}$ . Few nuclei show a slight worsening, in particular  $^{236}\text{U}$ ,  $^{238}\text{Pu}$ ,  $^{239}\text{Pu}$ ,  $^{242}\text{Pu}$ ,  $^{243}\text{Cm}$  and  $^{244}\text{Cm}$ . As before, the use of a 10% branching ratio for the  $(n,\gamma)$  reaction of  $^{241}\text{Am}$  produces a substantial improvement in the agreement of  $^{242\text{m}}\text{Am}$  and of  $^{242}\text{Cm}$  (which comes from  $\beta^-$  decay of  $^{242}\text{Am}$ ).

**Table XIII. Percent difference in the assembly-average concentrations in TRITON as compared to WIMS for the case of 44-MOX libraries and 10% <sup>241</sup>Am branching ratio**

	TRITON 44-UOX versus WIMS8			TRITON 44-MOX versus WIMS8		
	15 GWD/T	30 GWD/T	45 GWD/T	15 GWD/T	30 GWD/T	45 GWD/T
U-234	-5.40%	-5.70%	-5.70%	-5.00%	-5.20%	-5.20%
U-235	-0.70%	-1.80%	-2.90%	-0.60%	-1.70%	-2.70%
U-236	4.60%	4.20%	3.20%	4.60%	4.30%	3.40%
U-238	0.00%	0.00%	0.00%	0.00%	0.00%	0.00%
Pu-238	-0.10%	0.00%	0.90%	0.00%	0.30%	1.40%
Pu-239	0.50%	-2.60%	-3.20%	0.20%	-3.00%	-3.70%
Pu-240	-0.60%	-1.30%	-2.20%	-0.50%	-1.10%	-2.20%
Pu-241	0.60%	-0.50%	-1.50%	0.70%	-0.20%	-1.00%
Pu-242	1.50%	2.60%	3.80%	1.70%	3.00%	4.30%
Am-241	2.10%	1.60%	1.60%	1.30%	0.50%	0.20%
Am-242m	-13.10%	-0.30%	0.30%	-12.20%	-0.10%	0.10%
Am-243	0.20%	9.10%	12.30%	-4.70%	1.50%	2.80%
Cm-242	-3.90%	-1.90%	-1.70%	-2.10%	-0.70%	-0.90%
Cm-243	20.10%	20.80%	18.40%	23.00%	23.00%	19.90%
Cm-244	-13.90%	-5.00%	-1.50%	-1.50%	6.10%	7.80%
Cm-245	-34.20%	-29.40%	-29.50%	-24.10%	-20.60%	-22.50%

#### 4. CONCLUSIONS

The TRITON/NEWT sequence and associated cross section libraries of the SCALE 5.1 code package were found of satisfactory accuracy for modeling complex MOX-containing PWR fuel assemblies like the CORAIL, provided that the standard cross section 44 group library be modified to model properly the 1 eV <sup>240</sup>Pu resonance and that the ORIGEN default branching ratio for production of <sup>242m</sup>Am be changed to approximately 10-11%. A value of 10% for the branching ratio was found to provide good agreement with the calculated results of both APOLLO2 and WIMS8.

#### ACKNOWLEDGMENT

This work was supported by US DOE NERI under award number DE-FC07-06ID14736

#### REFERENCES

1. Gilles Youinou and Alfredo Vasile, Plutonium Multirecycling in Standard PWRs Loaded with Evolutionary Fuels, Nuclear Sci and Eng. 151, 25-45, 2005.
2. T.K.Kim et al. Benchmark Comparisons of Deterministic and Monte Carlo Codes for a PWR Heterogeneous Assembly Design, Physor 2004, Chicago, Ill, April 25-29.
3. SCALE: A Modular Code System for Performing Standardized Computer Analyses for Licensing Evaluation, ORNL/TM-2005/39, Version 5, Vols. I-III (April 2005). Available

from Radiation Safety Information Computational Center at Oak Ridge National Laboratory as CCC-725.

4. J.G.B. Saccheri, D.J. Diamond, A SCALE 5.0 Reactor Physics Assessment using the Module TRITON against Mixed Oxide (MOX) OECD/NEA benchmarks, Proceedings of the ICAPP '06, Reno NV USA June 4-8 2006, paper 6315.
5. CORAIL benchmark specifications-03, Nov 2003, internal communication.
6. O. Bringer, I. Al Mahamid, Ch. Blandin, S. Chabod, F. Chartier, E. Dupont, G.Fioni, H. Isnard, A. Letourneau, F. Marie, P. Mutti, L. Oriol, S. Panebianco, Ch.Veyssière, Detailed studies of Minor Actinide transmutation-incineration in high-intensity neutron Fluxes, PHYSOR-2006, Vancouver, BC, Canada, 2006, September 10-14.
7. Physics of Plutonium Recycling, Volume II, Nuclear Energy agency, Organization for Economic Co-Operation and Development, Paris, France 1995.
8. C. E. Sanders, I. C. Gauld, Isotopic Analysis of High-Burnup PWR Spent Fuel Samples From the Takahama-3 Reactor, NUREG/CR-6798.
9. F. GANDA and E. GREENSPAN, "OECD Benchmark A & B of MOX Fueled PWR Unit Cells Using SAS2H," These Transactions.